Journal of Sound and Vibration (2000) **230**(3), 689–707
doi:10.1006/jsvi.1999.2649, available online at http://www.idealibrary.com on IDEAL®

IDENTIFICATION OF COMPLEX MODULUS FROM MEASURED STRAINS ON AN AXIALLY IMPACTED BAR USING LEAST SQUARES

L. HILLSTRÖM, M. MOSSBERG AND B. LUNDBERG

The Ångström Laboratory, Uppsala University, P.O. Box 534, *SE*-751 21 *Uppsala, Sweden*
Department of Systems and Control, Uppsala University, P.O. Box 27, *SE*-751 03 *Uppsala, Sweden*

(*Received* 24 *February* 1999, *and in final form* 8 *September* 1999)

The complex modulus of a material with linearly viscoelastic behaviour is identified on the basis of strains which are known, from measurements and sometimes from a free end boundary condition, at three or more sections of an axially impacted bar specimen. The aim is to improve existing identification methods based on known strains at three uniformly distributed sections by increasing the number of sections considered and by distributing them non-uniformly. The increased number of sections results in an overdetermined system of equations from which an approximate solution for the complex modulus is determined using the method of least squares. Through the non-uniform distribution of sections, critical conditions with accompanying large errors at certain frequencies are largely eliminated. Experimental tests were carried out at room temperature with two materials, viz., polypropylene and polymethyl methacrylate, five strain gauge configurations and two kinds of impact excitation. Substantial improvement in the quality of the results for complex modulus was obtained.

© 2000 Academic Press

1. INTRODUCTION

In order to make efficient use of engineering materials with viscoelastic behaviour, it is imperative to know, and be able to determine, their complex moduli at relevant frequencies and temperatures. If such materials are to be used in components and structures which are loaded dynamically, e.g., through impact, then frequencies of interest may commonly vary from 100 Hz to 10 kHz. In this frequency range, wave propagation methods are well suited for the determination of complex modulus. Therefore, a number of such interrelated methods have been developed and used, mainly during the last two or three decades [1–13].

Axisymmetric viscoelastic waves in a uniform bar can be represented in the frequency domain by three complex-valued functions of frequency provided that the wavelengths are much larger than the diameter of the bar so that the conditions are approximately one-dimensional. One function is a wave propagation coefficient from which the complex modulus can be determined if the density of the material is

 © 2000 Academic Press

known. The real part of this function is the damping coefficient, and the imaginary part is the wavenumber. The remaining two functions represent the amplitudes of two waves which travel in opposite directions through the bar. Identification of the complex modulus requires data from which these three functions can be determined. This means that three independent measurements are normally required. However, the number of independent measurements can be reduced if the experimental conditions are such that one of the two waves can be measured at a time, or use can be made of a well-defined boundary condition such as that at a free end. A pair of independent measurements may concern one quantity, such as strain, at two different sections or two different quantities, such as force and acceleration, at one section.

Methods which are based on the measurement of one wave at a time have been employed in e.g., references [1–7]. An advantage of these methods is that they require only one (if a boundary condition is used) or two independent measurements. Another is their mathematical and computational simplicity. A disadvantage is that they may require relatively long bar specimens in order to keep waves travelling in opposite directions separate from each other at sections where measurements are made. Another disadvantage is that they may not be suitable for routine use, as some skill is required to ascertain that the condition of wave separation is fulfilled.

Methods which permit overlap of waves at instrumented sections have been used in, e.g., references [8–13]. Advantages of these methods are that they admit the use of relatively short bar specimens and have potential for use in routine testing. A disadvantage is that they require at least two (if a boundary condition is used) or three independent measurements. Another is that they may be mathematically and computationally complex. Thus, the equation which relates the wave propagation coefficient to the measured quantities normally has several or even a large number of solutions, and it is not always evident which one to choose. Also, numerical difficulties with resulting large errors and irregular results commonly occur at certain critical frequencies. One set of critical frequencies corresponds to conditions such that the distances between the sections considered become integral multiples of a half wavelength. If one quantity, such as strain, is measured at two sections, and the damping is low, then at the critical frequencies the harmonic components of the measured quantities have approximately equal magnitudes and phases which are either the same or opposite. This means that the two measurements are strongly correlated.

This paper concerns identification of complex modulus on the basis of strains which are known at three or more sections of an axially impacted bar specimen. Thus, overlap of waves at instrumented sections is allowed. The aim of the investigation is to improve existing identification methods [9, 11] based on known strains at $n = 3$ uniformly distributed sections. It is attempted to achieve this improvement by increasing the number of sections with known strains to $n > 3$ and by distributing them non-uniformly. The line of reasoning is as follows: Through the non-uniform distribution of sections, it should be possible to largely avoid that sections of each of several pairs are at critical distances from each other (i.e., an integral multiple of a half wavelength) at frequencies in the range of interest. At

frequencies where such coincidences cannot be avoided, the detrimental effects on the results of identification should be reduced due to the overdetermined system of equations which results from considering more than three sections (more than three equations for three unknown functions).

First, in Section 2, a one-dimensional model is presented and the identification problem is stated for an arbitrary number of sections with known strains $n \geqslant 3$. Then, in Section 3, identification procedures are presented for $n = 3$ and $n > 3$. Also, the sensitivity to errors in the measured strains is considered, and two types of critical conditions with corresponding critical frequencies are identified. Experimental tests carried out with $n = 3$ and 5 for polypropylene and with $n = 5$ for polymethyl methacrylate are presented in Section 4. In Sections 5 and 6, finally, results for wave propagation coefficients and complex moduli are presented and discussed. These results establish that substantial improvements in quality are obtained due to the increased number of sections considered and the non-uniform distribution of them.

2. MODEL AND STATEMENT OF PROBLEM

Consider a straight, uniform bar of linearly viscoelastic material with density ρ and complex modulus $E(\omega) = E'(\omega) + \mathrm{i}E''(\omega)$, where $\omega = 2\pi f$ is the angular frequency. The equation of axial motion of the bar can be expressed as

$$\partial^2\hat{\varepsilon}/\partial x^2 - \gamma^2\hat{\varepsilon} = 0, \tag{1}$$

where

$$\gamma^2(\omega) = -\rho\omega^2/E(\omega), \tag{2}$$

and $\hat{\varepsilon}(x, \omega) = \int_{-\infty}^{+\infty} \varepsilon(x, t)\mathrm{e}^{-\mathrm{i}\omega t}\mathrm{d}t$ is the Fourier transform of the axial strain $\varepsilon(x, t)$ at the section x and the time t.

The wave propagation coefficient $\gamma(\omega)$ is a complex-valued function, which can be expressed as $\gamma(\omega) = \alpha(\omega) + \mathrm{i}k(\omega)$ in terms of its real and imaginary parts. The damping coefficient $\alpha(\omega)$ is a positive even function, and the wavenumber $k(\omega)$ is an odd function, positive for $\omega > 0$ [14]. It is assumed that $k(\omega)$ is continuous, which implies $k(0) = 0$, and monotonically increasing. By definition, the wavelength can be obtained as $\lambda(\omega) = 2\pi/|k(\omega)|$. From the assumed properties of $k(\omega)$ it follows that $\lambda(\omega)$ is continuous and monotonically decreasing for $\omega > 0$ and that $\lambda(\omega) \to \infty$ as $\omega \to 0$. As the one-dimensional model represented by relations (1) and (2) requires that the wavelength $\lambda(\omega)$ should be much greater than the lateral dimensions d of the bar, only frequencies which are low enough to satisfy $\lambda(\omega) \gg d$, i.e., $|k(\omega)| \ll 2\pi/d$, are considered.

The general solution of equation (1) is

$$\hat{\varepsilon}(x, \omega) = \hat{P}(\omega)\mathrm{e}^{-\gamma(\omega)x} + \hat{N}(\omega)\mathrm{e}^{\gamma(\omega)x}, \tag{3}$$

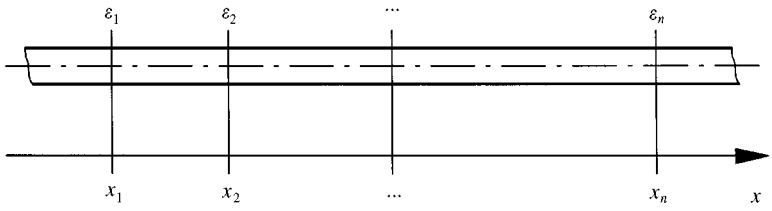

Figure 1. Sections with known strains.

where $\hat{P}(\omega)$ and $\hat{N}(\omega)$ are functions determined by initial and boundary conditions. From the inverse relation

$$\varepsilon(x,t) = (1/2\pi)\int_{-\infty}^{\infty} \hat{P}(\omega)\mathrm{e}^{-\alpha(\omega)x}\,\mathrm{e}^{\mathrm{i}[\omega t - k(\omega)x]}\,\mathrm{d}\omega$$

$$+ (1/2\pi)\int_{-\infty}^{\infty} \hat{N}(\omega)\mathrm{e}^{\alpha(\omega)x}\,\mathrm{e}^{\mathrm{i}[\omega t + k(\omega)x]}\,\mathrm{d}\omega \tag{4}$$

it can be seen that these functions represent the amplitudes at $x = 0$ of damped harmonic waves, which travel through the bar in the directions of increasing and decreasing x respectively.

Consider now n strains $\hat{\varepsilon}_1(\omega), \hat{\varepsilon}_2(\omega), \ldots, \hat{\varepsilon}_n(\omega)$ at sections $x_1 < x_2 < \cdots < x_n$ as shown in Figure 1. They are considered to be known either from n measurements or from $n - 1$ measurements and one boundary condition. If, e.g., there is a free end at section x_1, such a boundary condition is $\hat{\varepsilon}_1(\omega) \equiv 0$. From equation (3) it follows that the three complex-valued functions $\gamma(\omega)$, $\hat{P}(\omega)$ and $\hat{N}(\omega)$, considered to be unknown, are related to these strains and sections through the system of n equations

$$\mathbf{A}(\omega)\hat{\mathbf{w}}(\omega) = \hat{\boldsymbol{\varepsilon}}(\omega), \tag{5}$$

where

$$\mathbf{A}(\omega) = \begin{bmatrix} \mathrm{e}^{-\gamma(\omega)x_1} & \mathrm{e}^{\gamma(\omega)x_1} \\ \mathrm{e}^{-\gamma(\omega)x_2} & \mathrm{e}^{\gamma(\omega)x_2} \\ \vdots & \vdots \\ \mathrm{e}^{-\gamma(\omega)x_n} & \mathrm{e}^{\gamma(\omega)x_n} \end{bmatrix}, \quad \hat{\mathbf{w}}(\omega) = \begin{bmatrix} \hat{P}(\omega) \\ \hat{N}(\omega) \end{bmatrix}, \quad \hat{\boldsymbol{\varepsilon}}(\omega) = \begin{bmatrix} \hat{\varepsilon}_1(\omega) \\ \hat{\varepsilon}_2(\omega) \\ \vdots \\ \hat{\varepsilon}_n(\omega) \end{bmatrix}. \tag{6}$$

The problem to be considered is that of first determining the wave propagation coefficient $\gamma(\omega)$ from the system (5) and then, from equation (2), the complex modulus as

$$E(\omega) = -\rho\omega^2/\gamma^2(\omega). \tag{7}$$

Clearly, the number of known strains $\hat{\varepsilon}_1(\omega), \hat{\varepsilon}_2(\omega), \ldots, \hat{\varepsilon}_n(\omega)$ must be taken to be $n \geqslant 3$. For $n = 3$, there generally exists an exact solution of the system (5) for $\gamma(\omega)$ which also corresponds to the requirements on $\alpha(\omega)$ and $k(\omega)$ [9, 11]. At certain frequencies ω, however, there may not exist a solution and near such frequencies numerical solutions may be inaccurate. For $n > 3$, the system (5) is overdetermined. As the system is also afflicted with inaccuracies of the measurements and imperfections of the model, it generally has no exact solution for $\gamma(\omega)$ in this case. It will be shown, however, that normally the system has an approximate solution in the sense of least squares which also corresponds to the requirements on $\alpha(\omega)$ and $k(\omega)$. Next, the two cases $n = 3$ and $n > 3$ will be considered separately.

3. IDENTIFICATION AND SENSITIVITY TO ERRORS

3.1. THREE SECTIONS

Let $\hat{\varepsilon}_1$, $\hat{\varepsilon}_2$ and $\hat{\varepsilon}_3$, be known strains at the sections x_1, $x_2 = x_1 + ph$ and $x_3 = x_1 + qh$, where h is a characteristic length, p and q are relative primes (i.e., integers, which have no integer as a common factor) with $0 < p < q$. Thus, the ratios of the distances between any two of these sections are assumed to be rational numbers, which is no restriction in practice.

Elimination of $\hat{P}(\omega)$ and $\hat{N}(\omega)$ from the system (5) of $n = 3$ equations gives the equation

$$\hat{\varepsilon}_1(\xi^{q-p} - \xi^{p-q}) - \hat{\varepsilon}_2(\xi^q - \xi^{-q}) + \hat{\varepsilon}_3(\xi^p - \xi^{-p}) = 0, \tag{8}$$

with

$$\xi = \mathrm{e}^{\gamma h} \tag{9}$$

from which

$$\gamma h = \alpha h + \mathrm{i}kh, \quad \alpha h = \ln|\xi|, \quad kh = \arg(\xi) + m2\pi \tag{10}$$

are to be determined. In these relations $-\pi < \arg(\xi) \leqslant \pi$, and m is an integer to be chosen in such a way that $k(\omega)$ is a continuous and increasing function with $k(0) = 0$. The procedure for doing this, on the basis of measured strains which are afflicted with inaccuracies of measurement, is described in Appendix A.

If ξ is a root of equation (8), the ξ^{-1} is also a root. By relation (9), such a pair of roots corresponds to a pair $\pm\gamma$ of wave propagation coefficients with opposite signs. Therefore, only one of the two roots of such a pair is required for the description of the two waves represented by the right-hand side of relation (3). If $|\xi| > 1$ for one root of a pair and $|\xi| < 1$ for the other, then by relation (10) the latter root corresponds to $\alpha < 0$ and should be rejected. Also, if $|\xi| = 1$ for both roots of a pair, which corresponds to $\alpha = 0$, then one of them should be rejected.

Equation (8) has always a pair of roots $\xi = \pm 1$. By relation (10), this pair corresponds to $\alpha h = 0$ and $kh = r\pi$, where r is an integer. The first of these relations corresponds to elastic material and the second to wavelengths such that $h = r\lambda/2$, i.e., the distance h is an integral multiple of a half wavelength. This pair of roots has no relevance and should be rejected. This is done by first multiplying equation (8) by ξ^q, which makes the left-hand side a polynomial in ξ of degree $2q$, and then dividing by $\xi^2 - 1$. The result is the equation

$$\hat{\varepsilon}_1(\xi^{2q-p-2} + \xi^{2q-p-4} + \cdots + \xi^p) - \hat{\varepsilon}_2(\xi^{2q-2} + \xi^{2q-4} + \cdots + 1)$$

$$+ \hat{\varepsilon}_3(\xi^{q+p-2} + \xi^{q+p-4} + \cdots + \xi^{q-p}) = 0 \tag{11}$$

of degree $2(q-1)$ in ξ. The roots of this equation appear as $q-1$ pairs (ξ, ξ^{-1}). After rejection of one root of each pair, as justified above, there remain $q-1$ roots ξ. Only one of them is needed to describe the waves represented by the right-hand side of relation (3). When $q > 2$, therefore, it still remains to decide which root should be retained.

An unambiguous situation prevails when the integers p and q are minimal. As $0 < p < q$, this occurs when $p = 1$ and $q = 2$. Then, the sections are uniformly distributed (i.e., the distances between adjacent sections are the same), and equation (11) becomes

$$\hat{\varepsilon}_1\xi - \hat{\varepsilon}_2(\xi^2 + 1) + \hat{\varepsilon}_3\xi = 0. \tag{12}$$

This equation can be rewritten as $\xi^2 - 2\psi\xi + 1 = 0$ and has the two roots

$$\xi = \psi \pm (\psi^2 - 1)^{1/2}, \tag{13}$$

where

$$\psi = (1/2)(\hat{\varepsilon}_1 + \hat{\varepsilon}_3)/\hat{\varepsilon}_2. \tag{14}$$

The roots (13) form a single pair (ξ, ξ^{-1}), and only one of them, with $|\xi| \geqslant 1$, should be retained.

Relations (9), (13) and (14) define γh as a function of ξ, ξ as a function of ψ, and ψ as a function of $\hat{\varepsilon}_1$, $\hat{\varepsilon}_2$ and $\hat{\varepsilon}_3$ respectively. Thus, these relations define γh as a function $\Gamma(\hat{\varepsilon}_1, \hat{\varepsilon}_2, \hat{\varepsilon}_3)$, from which the sensitivities of γh to errors in $\hat{\varepsilon}_1$, $\hat{\varepsilon}_2$ and $\hat{\varepsilon}_3$, can be determined as

$$\frac{\partial\Gamma}{\partial\hat{\varepsilon}_1} = \frac{\partial\Gamma}{\partial\hat{\varepsilon}_3} = \frac{1}{2\hat{\varepsilon}_2(\psi^2 - 1)^{1/2}}, \quad \frac{\partial\Gamma}{\partial\hat{\varepsilon}_2} = \frac{\psi}{2\hat{\varepsilon}_2(\psi^2 - 1)^{1/2}} \tag{15}$$

respectively. The denominators of these expressions become zero when $\psi = \pm 1$ or $\hat{\varepsilon}_2 = 0$.

By relation (13), the condition $\psi = \pm 1$ corresponds to $\xi = \pm 1$, i.e., $\alpha h = 0$ and $kh = r\pi$, where r is an integer. As shown above, this critical condition occurs if the material is elastic and $h = r\lambda/2$ so that there is an integral multiple of a half wavelength in the distance h between two adjacent sections. If the material is viscoelastic instead, so that $\alpha h > 0$, while still

$$kh = r\pi, \quad h = r\lambda/2, \tag{16}$$

then by relations (9), (12) and (14) $\psi = \pm\cosh(\alpha h)$, and relations (15) yield

$$\left|\frac{\partial \Gamma}{\partial \hat{\varepsilon}_1}\right| = \left|\frac{\partial \Gamma}{\partial \hat{\varepsilon}_3}\right| = \frac{1}{2|\hat{\varepsilon}_2|\sinh(\alpha h)}, \quad \left|\frac{\partial \Gamma}{\partial \hat{\varepsilon}_2}\right| = \frac{1}{2|\hat{\varepsilon}_2|\tanh(\alpha h)}. \tag{17}$$

If the damping of waves in the distance h is low, then $\sinh(\alpha h) \approx \tanh(\alpha h) \approx \alpha h \ll 1$, and the denominators of the right-hand members of expressions (17) are small. Thus, if the conditions (16) prevail and the damping is low, then the magnitudes of the sensitivities (15) become large and the identification of the wave propagation coefficient γ and the complex modulus E can be expected to be inaccurate. The critical conditions (16) will be referred to as being of Type I.

The condition $\hat{\varepsilon}_2 = 0$ at $x_2 = a$ may arise if, e.g., there is a free end at $x = 0 \leqslant x_1$. Then, by relation (3) this occurs if $e^{2\gamma a} = 1$, which corresponds to $\alpha a = 0$ and $ka = s\pi$, where s is an integer. This critical condition occurs if the material is elastic and $a = s\lambda/2$ so that there is an integral multiple of a half wavelength in the distance a between the free end and the middle section x_2. If the material is viscoelastic instead, so that $\alpha h > 0$, while still

$$ka = s\pi, \quad a = s\lambda/2, \tag{18}$$

then by relation (3) $\hat{\varepsilon}_2 = \pm 2\hat{P}\sinh(\alpha a)$. Furthermore, by relations (9), (12) and (14) there is the result $\psi = (1/2)(\hat{\varepsilon}_1 + \hat{\varepsilon}_3)/\hat{\varepsilon}_2 = \cosh(\gamma h)$. Thus, relations (15) yield

$$\left|\frac{\partial \Gamma}{\partial \hat{\varepsilon}_1}\right| = \left|\frac{\partial \Gamma}{\partial \hat{\varepsilon}_3}\right| = \frac{1}{4|\hat{P}|\sinh(\alpha a)|\sinh(\gamma h)|}, \quad \left|\frac{\partial \Gamma}{\partial \hat{\varepsilon}_2}\right| = \frac{1}{4|\hat{P}|\sinh(\alpha a)|\tanh(\gamma h)|}. \tag{19}$$

If the damping is low in the sense that $\sinh(\alpha a) \approx \alpha a \ll 1$, then the denominators in expressions (19) become small and the identification of the wave propagation coefficient γ and the complex modulus E can be expected to be inaccurate. The critical conditions (18) will be referred to as being of Type II.

3.2. MORE THAN THREE SECTIONS

As there is generally no exact solution of the system (5) for $n > 3$, an approximate solution for $\hat{\mathbf{w}}$ and γ in the sense of least squares is determined by minimizing the

error

$$\tilde{e}(\hat{\mathbf{w}}, \gamma) = \|\mathbf{A}\hat{\mathbf{w}} - \hat{\boldsymbol{\varepsilon}}\| / \|\hat{\boldsymbol{\varepsilon}}\|, \tag{20}$$

where double bars denote the Euclidean norm (e.g., $\|\hat{\boldsymbol{\varepsilon}}\| = (|\hat{\varepsilon}_1|^2 + |\hat{\varepsilon}_2|^2 + \cdots + |\hat{\varepsilon}_n|^2)^{1/2}$). Thus, for each frequency ω, the error in the least-squares solution is

$$e = \min_{\hat{\mathbf{w}}, \gamma} \tilde{e}(\hat{\mathbf{w}}, \gamma). \tag{21}$$

The denominator in equation (20) is not necessary but makes the errors $\tilde{e}$ and e dimensionless and easy to interpret.

The minimization of $\tilde{e}(\hat{\mathbf{w}}, \gamma)$ is carried out in two steps as follows. First, this quantity is minimized with respect to $\hat{\mathbf{w}}$ for any γ by taking

$$\hat{\mathbf{w}} = \mathbf{A}^+ \hat{\boldsymbol{\varepsilon}} = (\mathbf{A}^*\mathbf{A})^{-1}\mathbf{A}^*\hat{\boldsymbol{\varepsilon}} = \hat{\mathbf{w}}_{LS}(\gamma), \tag{22}$$

where $\mathbf{A}^+ = (\mathbf{A}^*\mathbf{A})^{-1}\mathbf{A}^*$ is the Moore–Penrose pseudo-inverse matrix and $\mathbf{A}^* = \bar{\mathbf{A}}^{\mathrm{T}}$ is the adjoint (conjugate and transpose) matrix of $\mathbf{A}$. Then, $\tilde{e}(\hat{\mathbf{w}}_{LS}(\gamma), \gamma)$ is minimized numerically with respect to γ. The procedure for doing this, on the basis of measured strains afflicted with inaccuracies, is described in Appendix B.

In relation (22) it has been assumed that the matrix $\mathbf{A}^*\mathbf{A}$ can be inverted. In the particular case of uniformly distributed sections x_1, $x_2 = x_1 + h$, $x_3 = x_1 + 2h, \ldots, x_n = x_1 + (n-1)h$, one has

$$\det(\mathbf{A}^*\mathbf{A}) = \frac{1 - \cosh(2\alpha hn)}{1 - \cosh(2\alpha h)} - \frac{1 - \cos(2khn)}{1 - \cos(2kh)}, \tag{23}$$

from which it follows that $\det(\mathbf{A}^*\mathbf{A}) \to 0$ as $\alpha h \to 0$ and $kh \to r\pi$, where r is an integer. When $\alpha h = 0$ and $kh = r\pi$, all four elements of the matrix $\mathbf{A}^*\mathbf{A}$ become n, and $\det(\mathbf{A}^*\mathbf{A})$ becomes zero. Thus, if the material is elastic there are certain critical frequencies at which the matrix $\mathbf{A}^*\mathbf{A}$ has no inverse. Then there is no unique $\hat{\mathbf{w}}$ which minimizes $\tilde{e}(\hat{\mathbf{w}}, \gamma)$. This critical condition occurs, as before, if $h = r\lambda/2$ so that there is an integral multiple of a half wavelength in the distance h between adjacent sections. If the material is viscoelastic instead with low damping in the sense $0 < \alpha h < \alpha hn \ll 1$, while the conditions (16) still hold, then relation (23) can be replaced by

$$\det(\mathbf{A}^*\mathbf{A}) = \tfrac{1}{3}(n^2 - 1)(\alpha hn)^2 \ll n^2. \tag{24}$$

Thus, $\det(\mathbf{A}^*\mathbf{A})$ assumes values $\ll n^2$, while each element of $\mathbf{A}^*\mathbf{A}$ is approximately equal to n. This indicates possible numerical difficulties in carrying out step (22), and therefore conditions (16) of Type I are again critical. More generally, the sensitivity of the solution (22) to errors in $\mathbf{A}$ is expressed by the condition number $\mathrm{cond}(\mathbf{A}^*\mathbf{A}) = \lambda_{max}/\lambda_{min}$, where λ_{max} is the largest and λ_{min} the smallest eigenvalue of

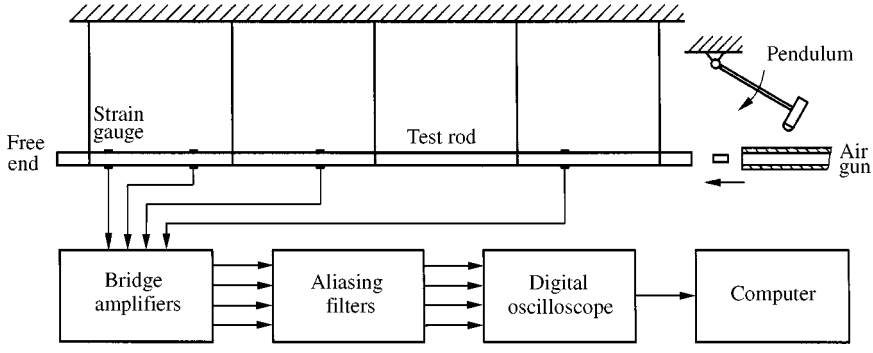

Figure 2. Experimental set-up.

the matrix $\mathbf{A}^*\mathbf{A}$. Under the same conditions as above one has the inequality

$$\operatorname{cond}(\mathbf{A}^*\mathbf{A}) = 12\,\frac{n^2}{n^2-1}\,\frac{1}{(\alpha h n)^2} \gg 1, \tag{25}$$

which is similar to equation (24).

4. EXPERIMENTS

The complex moduli were determined for two materials, viz., polypropylene (PP) and polymethyl methacrylate (PMMA) with densities 915 and 1183 kg/m^3 respectively. Two cylindrical test bars with circular cross-sections and length 2000 mm were used. The diameters were 16·6 mm for PP and 16·0 mm for PMMA.

The experimental set-up is illustrated in Figure 2. The test bars were suspended horizontally with thin wires and axially impacted either by a pendulum steel hammer or by a lead bullet from an air gun. The length of the hammer was 20 mm and its diameter was 10 mm. The impact end of the hammer was spherical with radius 10 mm. The length of the pendulum arm was 260 mm, and the pendulum was released from rest at its vertical position. The air gun (a rifle of Type Diana HDF Cal 4·5/0·177) was kept in horizontal position by a fixture. The bullets (Champion Olympic 0·177 cal/4·5 mm) had masses in the range 0·48–0·52 g and lengths in the range 5·8–6·1 mm.

Strain gauges (TML GFLA-6-350-70-1L) were glued (Tokyo Sokki Kenkyujo Co, Ltd, Adhesive CN) to the test bars in pairs with diametrically opposite members. Aron Poly Primer (Toagosei Chemical Industry Co., Ltd) was used for PP and Loctite 700 Polyolefin Primer (Cat. No. 77013) for PMMA. The gauges of each pair were connected to a bridge amplifier (Measurement Group 2210) in opposite branches so that contributions from small accidental bending strains were suppressed. Shunt calibration was used, and the bridge amplifiers were followed by aliasing filters (DIFA Measuring Systems, PDF) with cut-off frequency 35 kHz. The filtered signals were recorded by a four-channel digital oscilloscope (Nicolet Pro 20)

TABLE 1

Strain gauge configurations used in experimental tests

Strain gauge configuration	No. n of sections	No. of strain gauges	Use of free end	Distances of strain gauges from free end (mm)			
A	3	3	No	400	600	800	—
B	3	2	Yes	400	800	—	—
C	3	2	Yes	200	400	—	—
D	5	4	Yes	200	400	600	800
E	5	4	Yes	290	646	1078	1600

TABLE 2

Test conditions

Test	Material	Strain gauge configuration	Excitation	Temperature (°C)
1	PP	A	Pendulum	21·8
2	PP	B	Pendulum	21·8
3	PP	C	Pendulum	21·8
4	PP	D	Pendulum	21·8
5	PP	E	Pendulum	21·9
6	PP	E	Air gun	21·7
7	PMMA	E	Pendulum	22·1
8	PMMA	E	Air gun	22·2

with a sampling interval of 10 μs. The recorded signals were transferred to a computer for evaluation.

The five strain gauge configurations used in the tests, labelled A–E, are defined in Table 1. Configurations A–C made use of known strains at three sections ($n = 3$). In configuration A, the three strains were measured at distances x_1, x_2 and x_3 from the free end $x = 0$. In configurations B and C, use was made of a free end with zero strain at $x_1 = 0$, while strains were measured at sections x_2 and x_3. Configurations D and E made use of known strains at five sections ($n = 5$). In both of these configurations use was made of a free end with zero strain at $x_1 = 0$, while strains were measured at sections x_2, x_3, x_4 and x_5. Uniformly distributed sections were used in configurations A–D, while non-uniformly distributed ones were used in E. The five sections of the latter configuration were chosen so that the distances between two sections of each of the 10 possible pairs of sections approximately formed a geometric series.

The eight different tests carried out, labelled 1–8, are defined in Table 2. Tests 1–6 concerned PP, while Tests 7 and 8 involved PMMA. Other differences between the tests pertained to strain gauge configuration (A–E) and excitation (pendulum or air gun). All tests were carried out at room temperature in the range 21·7–22·2°C. This

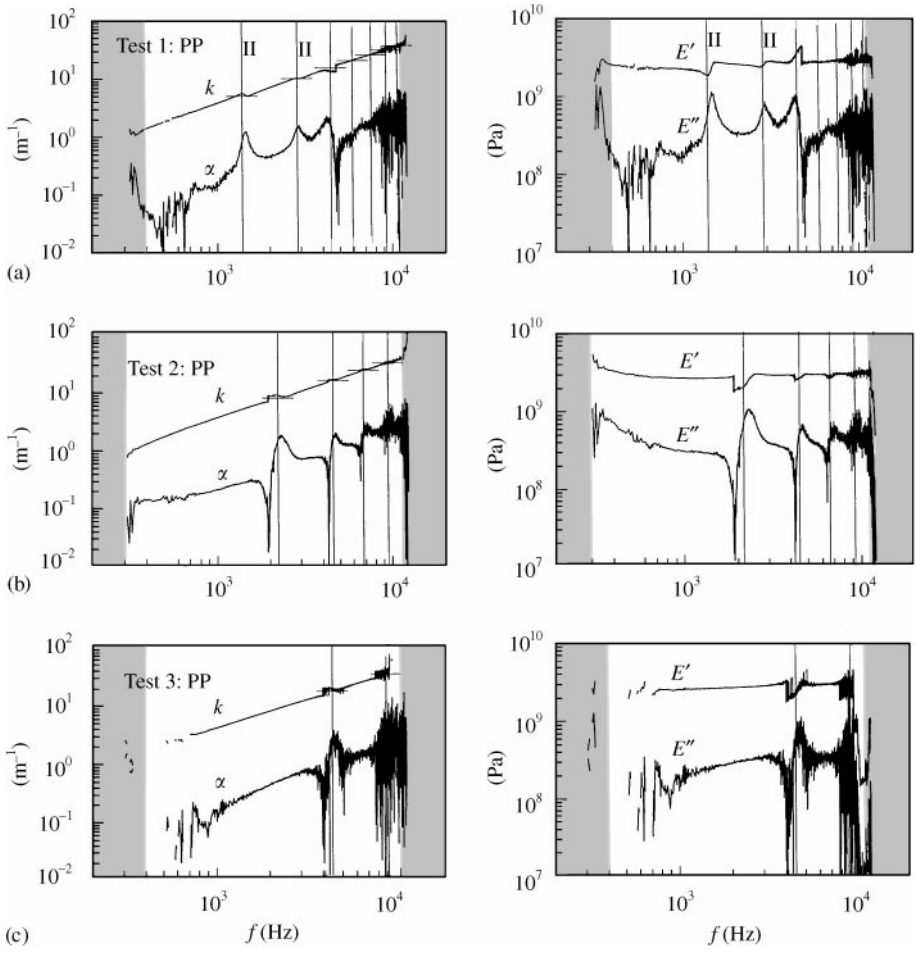

Figure 3. Wave propagation coefficient $\gamma = \alpha + \mathrm{i}k$ and complex modulus $E = E' + \mathrm{i}E''$ versus frequency f for polypropylene (PP) with critical frequencies marked by vertical lines. Where critical conditions of Types I or II are not indicated at a line, both prevail. Areas outside estimated useful frequency range are shaded. Three uniformly distributed sections; pendulum excitation. (a) Test 1: three measured strains; $h = 200$ mm. (b) Test 2: free end, two measured strains; $h = 400$ mm. (c) Test 3: free end, two measured strains; $h = 200$ mm.

means that in the range of frequencies of the tests of approximately 100 Hz–15 kHz both materials were in their glassy states.

5. RESULTS

The results from the tests are shown in Figures 3–7. Figures 3 (Tests 1–3) and 4 (Tests 4–6) show the wave propagation coefficient $\gamma = \alpha + \mathrm{i}k$ and the complex modulus $E = E' + \mathrm{i}E''$ versus frequency f for PP with critical conditions indicated by vertical lines. Figure 5 shows the error e versus frequency f in Tests 4–6 with PP. Figure 6 (Tests 7 and 8) shows the wave propagation coefficient $\gamma = \alpha + \mathrm{i}k$ and

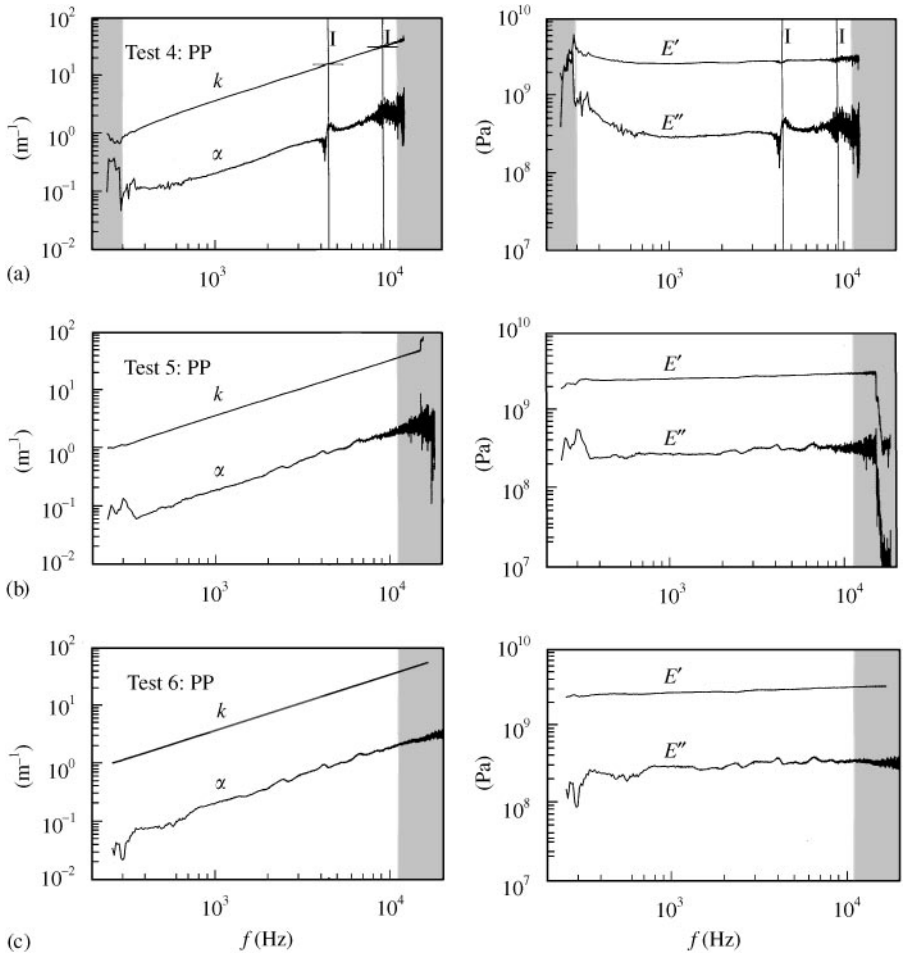

Figure 4. Wave propagation coefficient $\gamma = \alpha + \mathrm{i}k$ and complex modulus $E = E' + \mathrm{i}E''$ versus frequency f for polypropylene (PP) with critical frequencies marked by vertical lines. Areas outside estimated useful frequency range are shaded. Five sections; free end, four measured strains. (a) Test 4: uniformly distributed sections, $h = 200$ mm; pendulum excitation. (b) Test 5: non-uniformly distributed sections; pendulum excitation. (c) Test 6: non-uniformily distributed sections; air gun excitation.

complex modulus $E = E' + \mathrm{i}E''$ versus frequency f for PMMA. Figure 7 shows the error e versus frequency f in Tests 7 and 8 with PMMA.

The results of Tests 1–3 are plotted in the frequency interval 300 Hz to 12 kHz, while those of Tests 4–8 are plotted in the main frequency intervals where both α and k are positive. Also, in all tests, α, k, E' and E'' are plotted only at frequencies where each of these quantities is positive. This explains the interruptions in the plots of Tests 1–3.

6. DISCUSSION

A lower limit of useful frequencies can be estimated from the requirement that there must be sufficient variation of strain between the outermost sections x_1 and

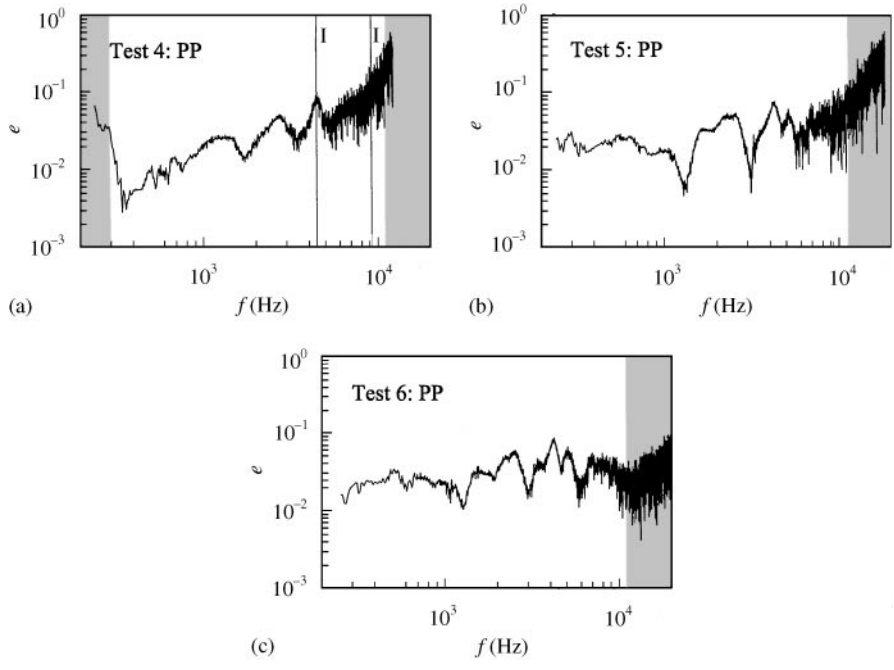

Figure 5. Error e versus frequency f for polypropylene (PP) with critical frequencies marked by vertical lines. Areas outside estimated useful frequency range are shaded. Five sections; free end, four measured strains. (a) Test 4: uniformly distributed sections, $h = 200$ mm; pendulum excitation. (b) Test 5: non-uniformly distributed sections; pendulum excitation. (c) Test 6: non-uniformly distributed sections; air gun excitation.

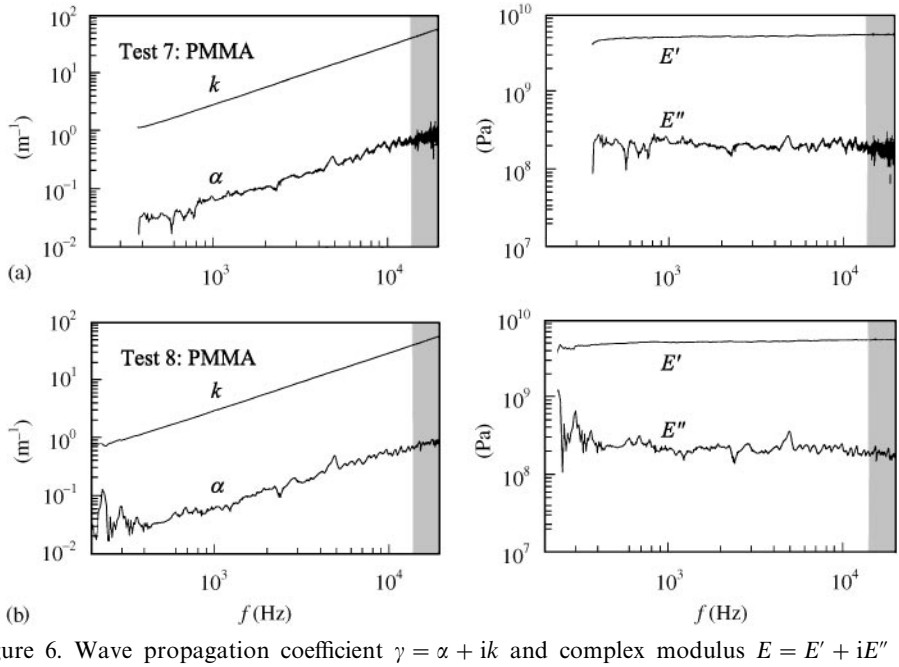

Figure 6. Wave propagation coefficient $\gamma = \alpha + \mathrm{i}k$ and complex modulus $E = E' + \mathrm{i}E''$ versus frequency f for polymethyl methacrylate (PMMA). Areas outside estimated useful frequency range are shaded. Five non-uniformly distributed sections; free end, four measured strains. (a) Test 7: pendulum excitation. (b) Test 8: air gun excitation.

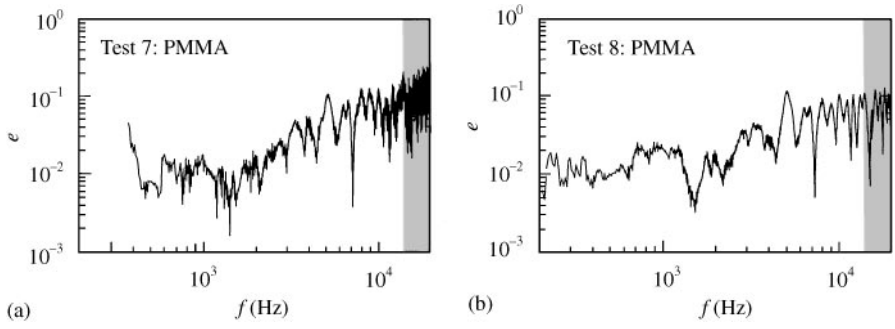

Figure 7. Error e versus frequency f for polymethyl methacrylate (PMMA). Areas outside estimated useful frequency range are shaded. Five non-uniformly distributed sections; free end, four measured strains. (a) Test 7: pendulum excitation. (b) Test 8: air gun excitation.

TABLE 3

Estimated lower and upper frequency limits

Test	Frequency limits	
	Lower (kHz)	Upper (kHz)
1, 3	0·4	11
2, 4	0·3	11
5, 6	0·1–0·2	11
7, 8	0·1–0·2	14

x_n. This implies wavelengths shorter than, say, ten times the distance between these sections. In Tests 1 and 3 this corresponds to wavenumbers above 1·6 m^{-1} and frequencies above 0·4 kHz. In Tests 2 and 4 the corresponding limits are 0·8 m^{-1} and 0·3 kHz, and in Tests 5–8, finally, they are 0·4 m^{-1} and 0·1–0·2 kHz. An upper limit of useful frequencies can be estimated from the requirement of the one-dimensional model used that the wavelength must be at least, say, 10 times the diameter of the bar specimen. In Tests 1–6 this implies wavenumbers below 38 m^{-1} and frequencies below 11 kHz. In Tests 7 and 8 the corresponding limits are 39 m^{-1} and 14 kHz. The estimated lower and upper frequency limits for the different tests are summarized in Table 3, and frequencies outside these limits are indicated by shaded areas in Figures 3–7. It can be seen from these figures that regions with irregular results extend into the estimated ranges of useful frequencies, i.e., into the ranges between the shaded areas. Thus, the ranges of useful frequencies are normally narrower than those estimated. This is believed to be due to factors which have not been considered, such as inadequate excitation and resulting insufficient signal-to-noise ratio at low and high frequencies.

It may seem possible to improve the identification of complex modulus by considering radial inertia in a similar way as was done by Love in the case of an isotropic elastic material. Then, the complex modulus given by equation (7) is modified by the multiplicative factor $[1 - \gamma^2(\omega)v^2(\omega)r_p^2]$, where $v(\omega)$ is the complex

equivalent of Poisson's ratio and r_p is the polar radius of gyration of the cross-section. However, this modification proves to be insignificant within the estimated ranges of useful frequencies, and outside these ranges it is of no use unless considerably better excitation can be achieved.

Strain gauge configurations A–C make use of known strains at three sections, which are uniformly distributed. For these configurations, the identification of complex modulus can be expected to be inaccurate at frequencies where any of the two types of critical conditions prevail. The first (Type I) occurs when there is an integral multiple of a half wavelength between any two sections, while the second (Type II) occurs when there is an integral multiple of a half wavelength between the free end of the bar specimen and the middle one of the three sections considered. At certain frequencies, the two types of critical condition may coincide. Strain gauge configuration A is similar to that used by Lundberg and Ödeen [11], while B and C are similar to those employed by Lundberg and Blanc [9].

Strain gauge configurations D and E make use of known strains at five different sections. This gives rise to an overdetermined system of equations for the wave propagation coefficient. For configuration D, in which the sections are uniformly distributed, conditions of Type I occur when the distance between any two sections is an integral multiple of a half wavelength. In configuration E, with non-uniformily distributed sections, there are 10 different distances between two sections. Therefore, critical conditions of Type I are unlikely and can occur only if these distances are integral multiples of a half wavelength. Numerical tests were carried out in order to investigate at which wavelengths and frequencies any two sections are at a distance from each other which, within 0·5 percent, is an integral multiple of a half wavelength. They showed that between the lower and upper frequency limits given in Table 3 for Tests 5–8, where configuration E was used, there are at most four pairs of sections out of 10 which are critical at a single frequency.

As can be seen in Figure 3, the results for PP obtained in Tests 1–3, with three uniformly distributed sections, are irregular at low frequencies, at high frequencies, and at frequencies where critical conditions of Types I or II prevail. The irregularities at low and high frequencies, inside the limits of Table 3, are largely due to insufficient signal-to-noise ratio achieved at these frequencies with the pendulum excitation. Therefore, these irregularities could be largely eliminated by forming averages from different tests. However, the irregularities associated with critical conditions of Types I or II were found to be repetitive, and therefore they could not be reduced in the same way. Regular results were obtained down to lower frequencies in Test 2 than in Tests 1 and 3 as estimated above.

The results for PP obtained in Tests 4–6, with five sections, are quite regular in a broad range of frequencies as can be seen in Figure 4. It can also be seen that regular results were obtained down to lower frequencies in Tests 5 and 6 than in Test 4, which is consistent with Table 3. The higher quality of the results in Test 6 than in Test 5 at high frequencies is believed to be due to better excitation achieved at high frequencies with the air gun than with the pendulum. In Test 4, with uniformly distributed sections, irregular results were obtained at only two frequencies where critical conditions of Type I prevailed. In Tests 5 and 6, with

non-uniformly distributed sections, there was no such irregularity. It can be noted that the improved quality of the results from Tests 4 to 5 and from Tests 5 to 6 is not unambiguously reflected by a corresponding reduction of the error e shown in Figure 5.

The results for PMMA obtained in Tests 7 and 8, with five non-uniformly distributed sections, are quite regular as can be seen in Figure 6. The slightly higher quality of the results from Test 8 than from Test 7 at low and high frequencies is believed to be due to the better excitation achieved with the air gun than with the pendulum. The slight improvement of quality from Tests 7 to 8 at high and low frequencies is reflected by a corresponding slight reduction of the error e shown in Figure 7.

The close agreement between the results obtained for PP in Test 5 with pendulum excitation (strain $\approx -0{\cdot}8 \times 10^{-3}$) and in Test 6 with air gun excitation (strain $\approx -3{\cdot}4 \times 10^{-3}$), and similarly for PMMA in Tests 7 (strain $\approx -0{\cdot}6 \times 10^{-3}$) and 8 (strain $\approx -2{\cdot}1 \times 10^{-3}$) respectively, indicates that the responses of both materials were linear under the conditions used in the tests. This linearity was assumed in the identification procedures used and is also a prerequisite for the definition of the complex modulus. A related parametric identification procedure for materials with non-linear viscoelastic response was developed by Trendafilova *et al.* [15].

According to the results shown in Figures 4(c) and 6(b), the loss angle $\delta = \arctan(E''/E')$ is typically 6–7° for PP and 2–3° for PMMA respectively, which means that PP is considerably more damping than PMMA. However, the results of Tests 6 (Figures 4 and 5) and 8 (Figures 6 and 7), which were carried out under the same conditions, show that this difference in damping had little effect on the regularity and the apparent quality of the results. This circumstance is believed to be due to the absence of critical conditions of Types I and II which results from the use of strain gauge configuration E (overdetermined system, non-uniform distribution). In the frequency interval 400 Hz–11 kHz, the real and imaginary parts of the complex moduli of the two materials show relatively little variation in the intervals 1–10 and 0·1–1 GPa respectively. Thus, for both materials the imaginary part of the complex modulus is about one order of magnitude less than the real part. The results for PP agree well with results obtained for the same material by Ödeen and Lundberg [10, 11].

In conclusion, the quality of the results for the complex modulus identified on the basis of measured strains at different sections of an axially impacted bar specimen has been improved significantly. This has been achieved mainly by increasing the number of sections with known strains to more than three, so that redundancy is introduced, and by using non-uniform rather than uniform distribution of sections, so that critical conditions are eliminated. As the four measurement channels needed in the tests (when used in combination with a free end boundary condition) are commonly provided by standard equipment, the price to be paid for the improved quality of results is not forbidding. Additional improvements have been obtained by using an air gun rather than a pendulum so that better excitation is achieved, especially at high frequencies. Similar improvements can be expected if other quantities than strain would be measured or if the excitation would be in torsion

(which would allow determination of the complex modulus in shear) rather than in compression.

A forthcoming paper will be devoted to a more extensive study of errors, including the effect of noise.

ACKNOWLEDGMENT

The authors want to thank Professor Torsten Söderström and Dr Bengt Carlsson, Department of Systems and Control, and Dr Leif Abrahamsson, Department of Scientific Computing, for ideas, remarks and other contributions which have resulted from co-operation within projects under contracts Dnr 96-212 and Dnr 98-137 funded by the Swedish Research Council for Engineering Sciences (TFR).

REFERENCES

1. H. Kolsky and S. S. Lee 1962 *Brown University Technical Report No.* 5. The propagation and reflection of stress pulses in linear viscoelastic media.
2. P. S. Theocaris and N. Papadopoulou 1978 *Polymer* **19**, 215–219. Propagation of stress waves in viscoelastic media.
3. R. H. Blanc 1971 *Doctoral Thesis, Université d'Aix-Marseille.* Détermination de l'équation de comportement des corps viscoélastiques linéaires par une méthode d'impulsion. Published in part in 1973 *Problèmes de la rhéologie* (W. K. Nowacki, editor), 65–85. Warsaw: IPPT PAN.
4. R. H. Blanc 1973 *Proceedings of the 2nd National Congress on Theoretical and Applied Mechanics, Varna, Bulgarian Academy of Science Publication, Sofia, 1976*, **2**, 555–564. Progress in pulse testing methods for viscoelastic solids.
5. R. H. Blanc 1993 *Journal of Applied Mechanics* **60**, 763–768. Transient wave propagation methods for determining the viscoelastic properties of solids.
6. Y. Sogabe, K. Kishida and K. Nakagawa 1982 *Bulletin of the Japan Society of Mechanical Engineers* **25**, 321–327. Wave propagation analysis for determining the dynamic properties of high damping alloys.
7. Y. Sogabe and M. Tsuzuki 1986 *Bulletin of the Japan Society of Mechanical Engineers* **29**, 2410–2417. Identification of the dynamic properties of linear viscoelastic materials by the wave propagation testing.
8. J. L. Buchanan 1987 *Journal of the Acoustical Society of America* **81**, 1775–1786. Numerical solution for the dynamic moduli of a viscoelastic bar.
9. B. Lundberg and R. H. Blanc 1988 *Journal of Sound and Vibration* **126**, 97–108. Determination of mechanical material properties from the two-point response of an impacted linearly viscoelastic rod specimen.
10. S. Ödeen and B. Lundberg 1993 *Journal of Sound and Vibration* **165**, 1–8. Determination of complex modulus from measured end-point accelerations of an impacted rod specimen.
11. B. Lundberg and S. Ödeen 1993 *Journal of Sound and Vibration* **167**, 413–419. *In situ* determination of the complex modulus from strain measurements on an impacted structure.
12. A. J. Hull 1996 *Journal of Sound and Vibration* **195**, 545–551. An inverse method to measure the axial modulus of composite materials under tension.
13. M. Soula, T. Vinh, Y. Chevalier, T. Beda and C. Esteoule 1997 *Journal of Sound and Vibration* **205**, 167–184. Measurements of isothermal complex moduli of viscoelastic materials over a large range of frequencies.

14. S. C. HUNTER 1960 *Progress in Solid Mechanics* (I. N. Sneddon and R. Hill, editors), **1**, 3–56. Amsterdam: North-Holland, Viscoelastic waves.
15. I. N. TRENDAFILOVA, S. ÖDEEN and B. LUNDBERG 1994 *European Journal of Mechanics A/Solids* **13**, 793–802. Identification of viscoelastic materials from electro-optical displacement measurements at two sections of an impacted rod specimen.

APPENDIX A: WAVENUMBER

It is assumed that the relevant complex root ξ_j from the solutions of equation (8) has been determined for each frequency ω_j. The dimensionless wavenumber $kh(\omega_j)$ is to be determined from this root and the last of relations (10) for all j. This is done by first calculating $kh(\omega_j) = \arg(\xi_j)$ for all j. In this way, values $kh(\omega_j)$ are obtained in the interval $-\pi < kh(\omega_j) \leqslant \pi$. These values are on an approximately saw-tooth shaped curve which has sudden jumps of approximately 2π between certain frequencies ω_j and ω_{j+1}. Then, for each $j = j_{\min}, \ldots, j_{\max}$, a term 2π is added to $kh(\omega_{j+1})$ iteratively so that the results, to the extent it is possible with regard to noise and measurement inaccuracies, become consistent with the requirements that the function $kh(\omega)$ should be continuous and increasing with $hk(0) = 0$. The criterion for adding 2π to $kh(\omega_{j+1})$ is that there should be a decrease $kh(\omega_j) - kh(\omega_{j+1})$ of at least $\kappa 2\pi$, where the coefficient κ is taken to be 0·5.

The algorithm used can be described as follows:

```
for j := j_min to j_max do
    begin
        kh(ω_j) := arg(ξ_j)
    end
flag := 1
while flag = 1 do
    begin
        flag := 0
        for j := j_min to j_max do
            begin
              if kh(ω_j) − kh(ω_{j+1}) > κ2π
                  then
                      begin
                          kh(ω_{j+1}) := kh(ω_{j+1}) + 2π
                          flag := 1
                      end
            end
    end
```

APPENDIX B: WAVE PROPAGATION COEFFICIENT

The wave propagation coefficient $\gamma(\omega_j)$ is to be determined so that the quantity $\tilde{e}(\hat{\mathbf{w}}_{LS}(\gamma), \gamma)$, obtained by substituting equation (22) into equation (21), is minimized for each angular frequency ω_j. This is done by using the MATLAB Version 5.2.1

function *fmins* which, starting from a suitably chosen starting value γ_{start} for each frequency ω_j, finds an adjacent value of γ which locally minimizes $\tilde{e}(\hat{\mathbf{w}}_{LS}(\gamma), \gamma)$ for the same frequency. The starting value γ_{start} for the first frequency ($\omega_{j_{\min}}$) is obtained through systematic search for an approximation of the value of γ which globally minimizes $\tilde{e}(\hat{\mathbf{w}}_{LS}(\gamma), \gamma)$. Starting values for subsequent frequencies up to $\omega_{j_{\max}}$ are obtained by choosing $\gamma_{start}(\omega_{j+1}) = \gamma(\omega_j)$. With this choice, it is assured that values $\gamma(\omega_j)$ are obtained which correspond to a continuous function $\gamma(\omega) = \alpha(\omega) + \mathrm{i}k(\omega)$.

The algorithm used can be described as follows:

```
set γ_start
for j := j_min to j_max do
    begin
        starting from γ = γ_start,
        find γ which locally minimizes ẽ(ŵ_LS(γ), γ)
        γ(ω_j) := γ
        γ_start := γ(ω_j)
    end
```

It is convenient to choose the first frequency $\omega_{j_{\min}}$ in the middle of the frequency range of interest, where the quality of measurements is the highest. Therefore, the for-loop is normally run once with frequencies decreasing ($\omega_{j_{max}} < \omega_{j_{min}}$) and once with frequencies increasing ($\omega_{j_{max}} > \omega_{j_{min}}$).